

## Measurements and Analyses of the $d_{5/2}$ Analog Resonance in the $^{88}\text{Sr}(p,n)^{88}\text{Y}$ Reaction\*

G. C. DUTT AND R. SCHRILS

*Department of Physics and Astronomy, University of Kentucky, Lexington, Kentucky 40506*

(Received 21 June 1968)

A study of the  $d_{5/2}$  isobaric analog resonance in the  $^{88}\text{Sr}(p,n)^{88}\text{Y}$  reaction is presented. Measurements of the cross section for the  $^{88}\text{Sr}(p,n_0)^{88}\text{Y}$  and  $^{88}\text{Sr}(p,n_1)^{88}\text{Y}$  reactions leaving the residual nucleus in the ground state and first excited state, respectively, have been made. Analyses of the analog resonance (at laboratory proton energy of 5.066 MeV) have been made using the coupled-channel formalism and the  $R$ -matrix approach of Robson. Good agreement with the experimental data has been obtained using both theories for this particular resonance.

### INTRODUCTION

ISOBARIC analog states are observed as compound-nucleus resonances in proton elastic scattering and proton-induced reactions in heavier nuclei.<sup>1</sup> These states are the isobaric analogs of the low-lying states of the nucleus formed by the addition of a neutron to the target. The occurrence of isobaric analog states was explained by Robson<sup>2</sup> using the isospin-dependent potential model of Lane.<sup>3</sup> In this formalism the interaction of the proton with the target nucleus is represented by a complex potential which includes a real isospin-dependent term. This results in a pair of coupled equations for the two states having isospin  $T_0 + \frac{1}{2}$  and  $T_0 - \frac{1}{2}$ , respectively, where  $T_0$  is the isospin of the target ground state.

The states with  $T_0 + \frac{1}{2}$  correspond to the low-lying states of the nucleus formed by the addition of a neutron to the target and occur at an excitation energy where the level density of the background states having  $T_0 - \frac{1}{2}$  is very high. Although the direct decay of the  $T_0 + \frac{1}{2}$  states into an outgoing neutron channel is forbidden by isospin selection rules, these states are mixed with the background states in this formalism, and thus neutron decay can occur.

The theory developed by Robson<sup>2</sup> for proton elastic scattering employs the  $R$ -matrix formalism and assumes that internal mixing is negligible. Robson *et al.*<sup>4</sup> extended the theory to  $(p,n)$  reactions and obtained good agreement to the  $^{92}\text{Zr}(p,n)$  experimental data, with the additional assumption that the analog state is dominated by the entrance channel. On the other hand, Johnson *et al.*<sup>5</sup> found that no quantitative agreement could be obtained between Robson's theory and

the experimental results for the  $3^-$  analog level in the  $(p,n)$  reaction on  $^{89}\text{Y}$ .

A different approach was employed by Tamura<sup>6</sup> and Auerbach *et al.*<sup>7</sup> for analyses of analog resonances occurring in the elastic scattering of protons from  $^{92}\text{Mo}$  and  $^{88}\text{Sr}$ , respectively. In this approach the coupled equations are solved explicitly. Good agreement with experimental results were obtained for the 5.3-MeV resonance in the case of  $^{92}\text{Mo}$  and the 5.06-, 6.06-, and 7.07-MeV resonances in the case of  $^{88}\text{Sr}$ . Auerbach *et al.*<sup>7</sup> emphasized in their analysis the need for measurements of absolute  $(p,n)$  cross sections in the neighborhood of the resonances as a further test of the model.

Kim and Robinson<sup>8</sup> have measured the relative excitation function at  $0^\circ$  for  $^{88}\text{Sr}(p,n)$  to the ground state of  $^{88}\text{Y}$  in the neighborhood of 5 MeV. Lightbody *et al.*<sup>9</sup> have measured the forward neutron yield (in relative units) to the ground state and first two excited states of  $^{88}\text{Y}$  in the same energy range. Both experiments show a strong resonance in the yield curve of the neutrons which leave  $^{88}\text{Y}$  in its ground state (the  $n_0$  group), at around 5.1 MeV. Angular distributions for this group were measured on and off resonance by Lightbody *et al.*<sup>9</sup>

The present work describes the measurements of absolute  $^{88}\text{Sr}(p,n)$  cross sections in the neighborhood of the 5.1-MeV resonance. Analyses involving both the explicit solution of the coupled equations and the method of Robson are presented.

### EXPERIMENTAL METHODS

Targets of strontium oxide (enriched to 99% in  $^{88}\text{Sr}$ ), evaporated on 0.005-in. thick gold backings, were bombarded by protons accelerated in the University of Kentucky 5.5-MeV Van de Graaff accelerator. The neutrons from the  $^{88}\text{Sr}(p,n)^{88}\text{Y}$  reaction were detected by an NE 213 liquid scintillator. Standard

\* Research supported in part by the National Science Foundation.

<sup>1</sup> J. D. Fox, C. F. Moore, and D. Robson, *Phys. Rev. Letters* **12**, 198 (1964); P. Richard, C. F. Moore, D. Robson, and J. D. Fox, *ibid.* **13**, 343 (1964); see also Ref. 5 and various papers in *Isobaric Spin in Nuclear Physics*, edited by J. D. Fox and D. Robson (Academic Press Inc., New York, 1966).

<sup>2</sup> D. Robson, *Phys. Rev.* **137**, B535 (1965).

<sup>3</sup> A. M. Lane, *Nucl. Phys.* **35**, 676 (1962).

<sup>4</sup> D. Robson, J. D. Fox, P. Richard, and C. F. Moore, *Phys. Letters* **18**, 86 (1965).

<sup>5</sup> C. H. Johnson, R. L. Kernell, and S. Ramaratnam, *Nucl. Phys.* **A107**, 21 (1968).

<sup>6</sup> T. Tamura, in *Isobaric Spin in Nuclear Physics*, edited by J. D. Fox and D. Robson (Academic Press Inc., New York, 1966), p. 447.

<sup>7</sup> E. H. Auerbach, C. B. Dover, A. K. Kerman, R. H. Lemmer, and E. H. Schwarcz, *Phys. Rev. Letters* **17**, 1184 (1966).

<sup>8</sup> H. J. Kim and R. L. Robinson, *Phys. Rev.* **151**, 920 (1966).

<sup>9</sup> D. B. Lightbody, A. Sayres, and G. E. Mitchell, *Phys. Rev.* **153**, 1214 (1967).

time-of-flight techniques were used to separate the different neutron groups. For this purpose the proton beam was pulsed at the accelerator terminal into bursts of 7 nsec duration. Using a flight path of 1.5 m it was possible to separate the different neutron groups. In order to observe the low-energy neutron groups leaving the residual nucleus in its excited states, the bias of the neutron detector was set at an energy equivalent of 50-keV protons. This was made possible by arranging two photomultipliers to view the same scintillator and taking coincidences between the two photomultiplier signals to eliminate noise. To reduce background, the detector assembly was placed in a shield of lithium carbonate and paraffin, described previously by Reber and Brandenberger.<sup>10</sup>

The thickness of the target was measured by counting the number of protons elastically scattered at  $140^\circ$  from a target of  $^{88}\text{SrO}$ , evaporated on a 0.005-in.-thick aluminum backing. The incident proton energy was lowered to 2 MeV for this measurement and at this energy the elastic scattering was assumed to be pure Coulomb scattering. At 2-MeV proton energy and at  $140^\circ$  scattering angle, the protons elastically scattered from  $^{88}\text{Sr}$  were separated from those scattered from

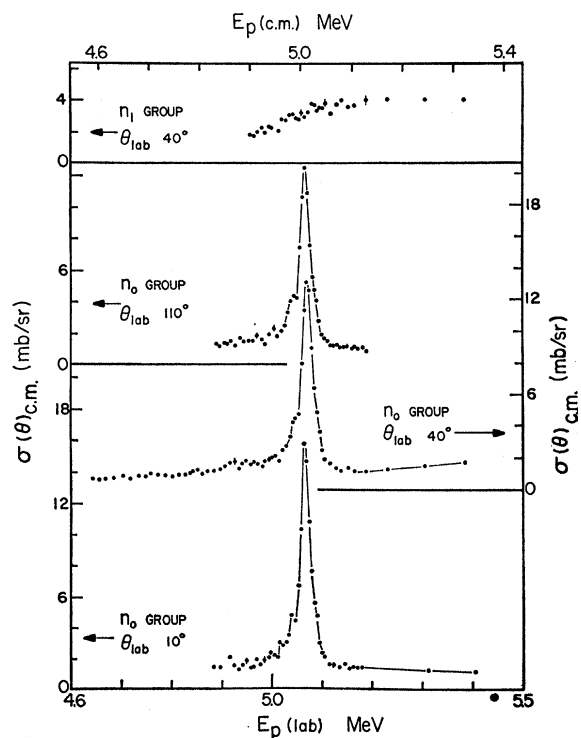


FIG. 1. Excitation functions of the  $^{88}\text{Sr}(p,n_0)^{88}\text{Y}$  and  $^{88}\text{Sr}(p,n_1)^{88}\text{Y}$  reactions. The lower three curves are for the ground-state group neutrons at the angles indicated. The top curve is for the first-excited-state group neutrons. The target thickness used was about 6 keV for 5-MeV protons.

<sup>10</sup> J. D. Reber and J. D. Brandenberger, Phys. Rev. **163**, 1077 (1967).

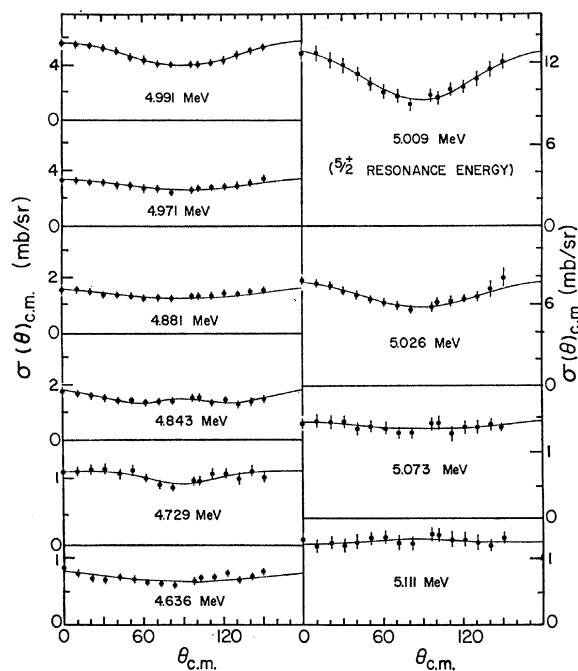


FIG. 2. Angular distributions of the neutrons from the  $^{88}\text{Sr}(p,n_0)^{88}\text{Y}$  reactions. The c.m. proton energies are shown in the respective figures. The target thickness used was about 10 keV for 5-MeV protons.

oxygen and aluminum. From these measurements the thickness of the target was calculated using the Rutherford scattering formula. Then the thickness of the gold-backed targets, which were used in the main experiment, were calculated by comparing the neutron yield from this target to the yield from the standard aluminum-backed target. The thickness of the target calculated in this way agreed to within 10% with the thickness obtained from weighing.

The neutron detection efficiency of the scintillation detector was measured by comparison with a long counter using monoenergetic neutrons from the  $^7\text{Li}(p,n)$  and  $\text{T}(p,n)$  reactions. The relative efficiency of the long counter was taken from the work of Allen *et al.*<sup>11</sup> The absolute efficiency of the long counter was measured using a Pu-Be neutron source, whose absolute neutron-emission rate was calibrated at the National Bureau of Standards. The uncertainty in the absolute neutron-detection efficiency of the neutron detector is estimated to be not more than 10%. The relative and absolute uncertainties in the measured cross sections are estimated to be  $\pm 8$  and  $\pm 20\%$ , respectively.

## RESULTS

Figure 1 shows excitation functions of the  $^{88}\text{Sr}(p,n_0)^{88}\text{Y}$  and  $^{88}\text{Sr}(p,n_1)^{88}\text{Y}$  reactions leaving the residual nucleus  $^{88}\text{Y}$  in its ground state ( $J^\pi = 4^-$ ) and the first excited state at 0.394 MeV ( $J^\pi = 1^+$ ), respectively.

<sup>11</sup> W. D. Allen and A. T. G. Ferguson, Proc. Phys. Soc. (London) **70A**, 639 (1957).

The resonance at  $5.066 \pm 0.01$  MeV seen in the excitation functions for the  $n_0$  group is due to the isobaric analog state in  $^{89}\text{Y}$  which corresponds to the ground state of  $^{89}\text{Sr}(J^\pi = \frac{5}{2}^+)$ . This state is formed by  $d_{5/2}$  protons incident on the target  $^{88}\text{Sr}(J^\pi = 0^+)$ . The experimental width of the resonance is 22 keV. The resonance shows the assymetry which is predicted by the theory of Robson.<sup>4</sup> This analog state is not seen in the  $n_1$  group excitation function. A similar situation occurs in the  $^{89}\text{Y}(p, n)^{89}\text{Zr}$  reaction and was attributed to the lower penetrability of the outgoing neutron leaving the residual nucleus in the excited state.<sup>12</sup>

Figure 2 shows the angular distributions of the neutrons leaving the residual nucleus in its ground state, at 10 c.m. proton energies ranging from 4.636 to 5.111 MeV. In the c.m. system the resonance occurs at 5.009 MeV.

Figure 3 shows the angular distributions of the  $n_1$  group neutrons at c.m. proton energies around the resonance. All the angular distributions are symmetric about  $90^\circ$ , within the experimental error, which is consistent with the statistical theory of nuclear reactions. The solid curves shown in Figs. 2 and 3 are the least-squares fit to Legendre polynomials using  $P_0$ ,  $P_2$ , and  $P_4$  only.

## ANALYSIS

### A. Coupled-Channel Formalism

The occurrence of isobaric analog resonances in proton-induced reactions may be described by the pair of coupled equations (1) and (2), in the upper ( $T^+ = T_0 + \frac{1}{2}$ ) and lower ( $T^- = T_0 - \frac{1}{2}$ ) isospin-state representation.<sup>2</sup> Here  $T_0$  and  $\frac{1}{2}$  are the isospins of the target and

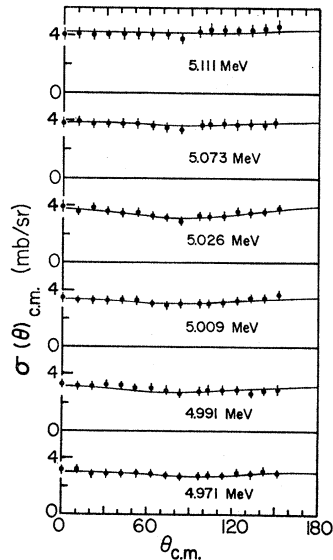


Fig. 3. Angular distributions of the neutrons from the  $^{88}\text{Sr}(p, n_1)^{88}\text{Y}$  reaction leaving  $^{88}\text{Y}$  in the first excited state. The c.m. proton energies are shown in the respective figures. The target thickness used was about 10 keV for 5-MeV protons.

<sup>12</sup> G. S. Mani and G. C. Dutt, Phys. Letters 16, 50 (1965).

proton, respectively.

$$\left\{ \frac{\hbar^2}{2m} \frac{d^2}{dr^2} + E - \Delta - V^+ - \frac{1}{2} T_0 U - \frac{\hbar^2 l(l+1)}{2mr^2} \right\} \chi^+ = \frac{V_c - \Delta}{2T_0 + 1} \{ \chi^+ + (2T_0)^{1/2} \chi^- \}, \quad (1)$$

$$\left\{ \frac{\hbar^2}{2m} \frac{d^2}{dr^2} + E - V_c - V^- + \frac{1}{2} (T_0 + 1) U - \frac{\hbar^2 l(l+1)}{2mr^2} \right\} \chi^- = \frac{V_c - \Delta}{2T_0 + 1} \{ (2T_0)^{1/2} \chi^+ - \chi^- \}. \quad (2)$$

In Eqs. (1) and (2) the first term on the left-hand side is the kinetic energy and the last one is the centrifugal term;  $E$  is the proton energy;  $\Delta$  is the Coulomb displacement energy between the target state and its analog;  $V_c$  is the one-body Coulomb potential of the proton in the target;  $\chi^+$  and  $\chi^-$  are the channel functions in the  $T^+$  and  $T^-$  channels, respectively;  $U$  is the isospin potential, explicitly

$$U = U_0 j(r); \quad (3)$$

$V^+$  and  $V^-$  are the complex potentials in the  $T^+$  and  $T^-$  channels, respectively, shown in Eqs. (4) and (5).

$$V^+ = -V_0 f(r) - V_{so} \sigma \cdot \mathbf{h}(r) - iW^+, \quad (4)$$

$$V^- = -V_0 f(r) - V_{so} \sigma \cdot \mathbf{h}(r) - iW^-, \quad (5)$$

where

$$W^+ = W_0^+ g(r), \quad W^- = W_0^- g(r),$$

$$f(r) = [1 + \exp((r-R)/a)]^{-1},$$

$$g(r) = -4b(d/dr)[1 + \exp((r-R)/b)]^{-1},$$

$$h(r) = -\lambda_\pi^2 r^{-1} [df(r)/dr],$$

$\lambda_\pi$  being the pion compton wavelength, and

$$j(r) = \exp(-(r-R)^2/a^2).$$

The real part  $V_0$  and the spin orbit  $V_{so}$  of the complex potential are taken to be the same in the  $T^+$  and  $T^-$  channels. But the imaginary part  $W_0$  is expected to be different in the two channels. The  $T^+$  channel corresponds to the low-lying states of the neutron analog and hence  $W_0^+$  is expected to be very small or zero.<sup>7</sup>

On transforming Eqs. (1) and (2) into the physical channels, proton plus target ( $|pC\rangle$ ) and neutron plus analog of the target ( $|nA\rangle$ ), Eqs. (6) and (7) are obtained<sup>13</sup>:

$$\left\{ \frac{\hbar^2}{2m} \frac{d^2}{dr^2} + E - V_c - V_{\text{real}}^- + \frac{1}{2} T_0 U - \frac{\hbar^2 l(l+1)}{2mr^2} + \frac{i(W^+ - W^-)}{2T_0 + 1} \right\} \chi_p = \frac{2i(W^- - W^+)}{2T_0 + 1} \chi_n, \quad (6)$$

<sup>13</sup> That fact that there are differences among Eqs. (6) and (7) and the corresponding equations which appear in Refs. 6 and 7 is due to misprints in the latter.

$$\left\{ \frac{\hbar^2}{2m} \frac{d^2}{dr^2} + E - \Delta - V_{\text{real}} + \right. \\ \left. - \frac{1}{2}(T_0 - 1)U - \frac{\hbar^2 l(l+1)}{2mr^2} + \frac{i(W^- - W^+)}{2T_0 + 1} \right\} \chi_n \\ = \left( \frac{1}{2}T_0 \right)^{1/2} \left\{ U + \frac{2i(W^- - W^+)}{2T_0 + 1} \right\} \chi_p. \quad (7)$$

In Eqs. (6) and (7)  $\chi_p$  and  $\chi_n$  are the wave functions in the  $|pC\rangle$  and  $|nA\rangle$  channels, respectively. For proton energies  $E < \Delta$ ,  $\chi_n$  is in a negative energy state. Because of the coupling between the  $|pC\rangle$  and  $|nA\rangle$  channels, resonances are produced in the  $|pC\rangle$  system at energies corresponding to the bound states of the  $|nA\rangle$  system.

The solutions of Eqs. (6) and (7), after matching to the appropriate external wave functions, yield the scattering function  $S$ . As in the usual complex potential model, the potential scattering cross section is proportional to  $|1 - S|^2$  and the absorption cross section is proportional to  $1 - |S|^2$ . It is usual in proton complex potential model calculations to neglect compound-elastic scattering, when many neutron channels are open, because of the lower penetrability of protons. But this is no longer true when there is enhancement of the cross section at the analog resonance, as in the case presented here. The absorption cross section at the peak of the resonance is several times the background cross section and hence competition from proton reemission cannot be neglected. The compound-elastic scattering

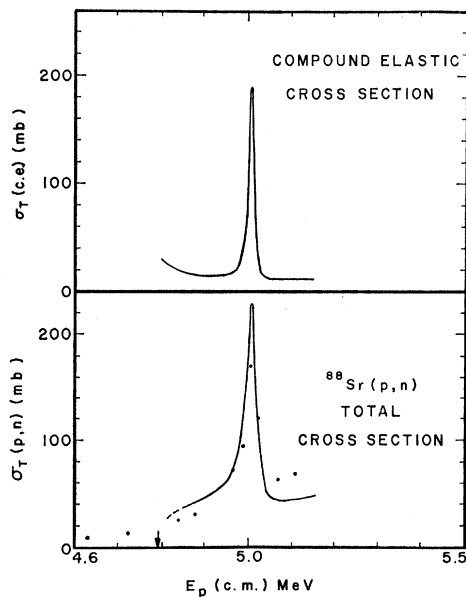


FIG. 4. The  $(p,n)$  total cross section and the compound elastic cross section in the  $^{88}\text{Sr} + p$  reaction. The curves are the results of the coupled-channel calculations. The points in the lower figure are the experimental data. The arrow refers to the threshold for the  $^{88}\text{Sr}(p,n)^{88}\text{Y}$  reaction.

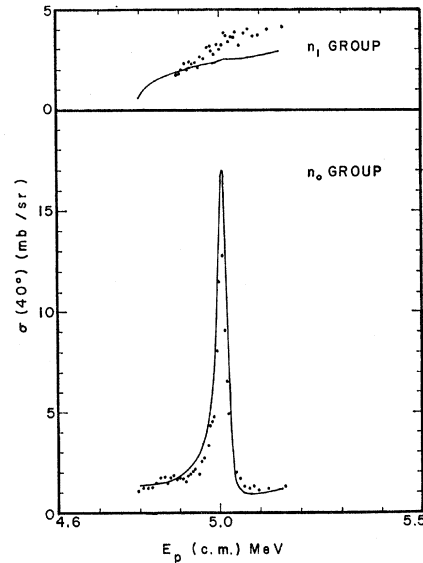


FIG. 5. The differential cross section, at  $40^\circ$ , for the  $^{88}\text{Sr}(p,n_0)^{88}\text{Y}$  and the  $^{88}\text{Sr}(p,n_1)^{88}\text{Y}$  reactions. The curves are the results of the coupled-channel calculations. The points are the experimental data.

must be subtracted from the absorption cross section before comparison with the  $(p,n)$  experimental cross section is made. In calculating  $(p,p)$  differential cross sections, the compound-elastic cross section must also be taken into account. However, in that case its effect is negligible compared to the shape-elastic and Coulomb cross sections and the interference between these.

The statistical theory of nuclear reactions is appropriate to calculate the compound-elastic scattering cross section. In this model the cross section for a reaction from channel  $a$  to channel  $b$  is the product of the absorption cross section in channel  $a$  and the probability of decay of the compound nucleus into channel  $b$ , i.e.,

$$\sigma(a,b) = \sigma_{ab}(a) T(b) / \sum_c T_c,$$

where  $\sigma_{ab}(a)$  is the absorption cross section in channel  $a$  and the  $T$ 's are the complex potential transmission coefficients.

Equations (6) and (7) were used in conjunction with the statistical model to numerically calculate the  $^{88}\text{Sr}(p,n)$  cross section in the vicinity of the  $\frac{5}{2}^+$  isobaric analog resonance at 5.066 MeV laboratory proton energy. Figure 4 shows the calculated  $(p,n)$  total cross section and the compound-elastic cross section. The data points in the  $(p,n)$  cross-section curve are the experimental cross sections integrated over all angles and summed over the two open neutron channels corresponding to the ground state and the first excited state of the residual nucleus. Figure 5 shows the comparison of the calculated differential cross section for the  $^{88}\text{Sr}(p,n_0)$  and the  $^{88}\text{Sr}(p,n_1)$  reactions at an angle of  $40^\circ$ , with the experimental data shown as points.

The following complex potential parameters were used in the coupled channel calculations, in the notations of Eqs. (3)–(5):

$$\begin{aligned} V_0(l \neq 2) &= 53.09 \text{ MeV}, & V_0(l=2) &= 52.573 \text{ MeV}, \\ R &= 1.25A^{1/3} \text{ fm}, & a &= 0.65 \text{ fm}, & b &= 0.47 \text{ fm}, \\ W_0^- &= 5 \text{ MeV}, & W_0^+ &= 0.005 \text{ MeV}, \\ V_{s_0} &= 5.65 \text{ MeV}, & U_0 &= 2.2 \text{ MeV}, & \Delta &= 11.45 \text{ MeV}. \end{aligned}$$

These parameters are the same as those used by Auerbach *et al.*<sup>7</sup> to fit the  $^{88}\text{Sr}(p,p)$  data, except for  $V_0$  and  $W_0$ . The  $V_0$ 's used here are  $\sim 2$  MeV lower than those used in Ref. 7. We have found it necessary to use these values of  $V_0$  to position the resonances in the  $^{88}\text{Sr}+p$  reactions at the observed energies. Auerbach *et al.*<sup>1</sup> used an imaginary term  $W_0 (= 3 \text{ MeV})$  in the complex potential only in the  $T^-$  channel, but pointed out that a fit to the  $^{88}\text{Sr}(p,n)$  cross section would determine  $W_0$  more precisely. We used  $W_0^- = 5 \text{ MeV}$  and also included a small imaginary potential  $W_0^+ (= 0.005 \text{ MeV})$  in the  $T^+$  channel. These values for  $W_0^-$  and  $W_0^+$  were chosen to get a good visual fit to the  $^{88}\text{Sr}(p,n)$  data, and at the same time not significantly disturb the elastic scattering fit. The effect of increasing  $W_0^+$  to any value much beyond 5 keV is to considerably lower the resonance peak, making its width greater. Choosing  $W_0^+ = 0$  does not affect the  $(p,p)$  fit, but slightly worsens the  $(p,n)$  fit. Figure 6 shows the calculated  $^{88}\text{Sr}(p,p)$  differential cross section at  $90^\circ$  compared to the experimental points, from Cosman *et al.*<sup>14</sup>

For the exit channels, the complex potential parameters used in this calculation for neutrons are those of Moldauer.<sup>15</sup> For the inelastic proton channels, the complex potential parameters of Johnson *et al.*<sup>16</sup> were used.

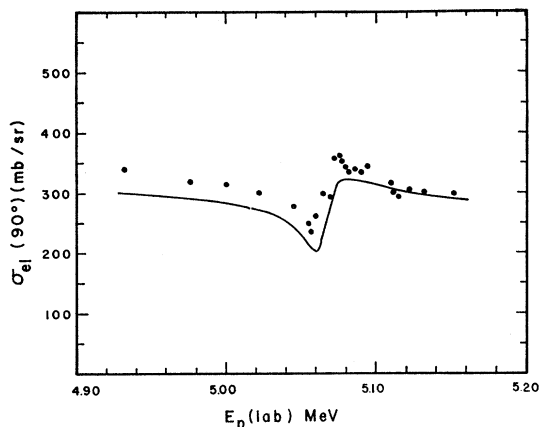


FIG. 6. The differential cross sections for  $^{88}\text{Sr}(p,p)^{88}\text{Sr}$  scattering. The curve is the result of the coupled-channel calculation. The points are the experimental data taken from Cosman *et al.* (Ref. 14).

<sup>14</sup> E. R. Cosman, H. A. Enge, and A. Sperduto, Phys. Letters **22**, 195 (1966).

<sup>15</sup> P. A. Moldauer, Phys. Rev. Letters **9**, 17 (1962).

<sup>16</sup> See page 26 of Ref. 5.

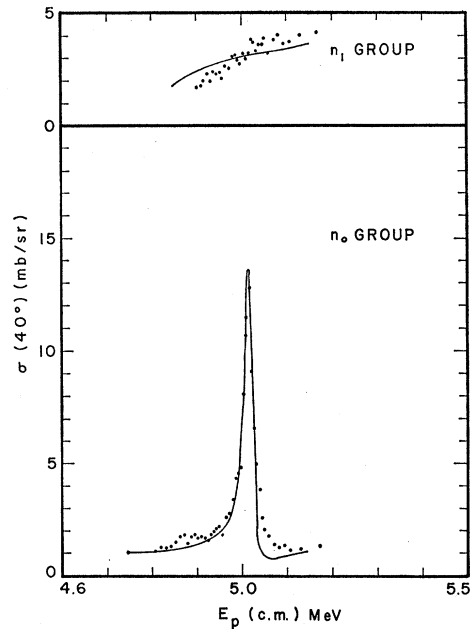


FIG. 7. The differential cross section, at  $40^\circ$ , for the  $^{88}\text{Sr}(p,n_0)^{88}\text{Y}$  and the  $^{88}\text{Sr}(p,n_1)^{88}\text{Y}$  reactions. The curves are the results of the calculation using Robson's theory. The points are the experimental data. See text for values of parameters used.

## B. Robson's Theory

As previously mentioned, Robson *et al.*<sup>4</sup> have formulated a theory of analog resonances in  $(p,n)$  reactions, using the  $R$ -matrix formalism on the assumptions that the analog state is dominated by a single channel and that internal mixing can be neglected. The assumption that the resonance is dominated by the incident proton channel is expected to be good in the case of  $^{88}\text{Sr}$ , which has 50 neutrons and 38 protons, corresponding to closed  $1g_{9/2}$  and  $1f_{5/2}$  shells, respectively. Under these assumptions, the  $(p,n)$  cross section, for states of the same spin and parity as the analog state, is proportional to

$$T_p^{\text{EN}} T_n / \sum_c T_c,$$

where  $T_p^{\text{EN}}$  is the enhanced transmission coefficient in the proton channel,  $T_n$  is the transmission coefficient in the neutron channel,  $T_c$  is the transmission coefficient in channel  $c$ , and the summation includes all open channels.  $T_p^{\text{EN}}$  is given by

$$T_p^{\text{EN}} = T_p (E - E_0 + \Delta)^2 / (E - E_0)^2 + \frac{1}{4} \Gamma^2,$$

where  $T_p$  is the complex potential transmission coefficient,  $E$  is the c.m. proton energy,  $E_0$  is the resonance energy,  $\Delta$  is the level shift, and  $\Gamma$  is the resonance width.

Figure 7 shows the calculated differential cross sections for the  $^{88}\text{Sr}(p,n_0)$  and  $^{88}\text{Sr}(p,n_1)$  reactions at an angle of  $40^\circ$ , using Robson's theory. The points are the experimental data. Figure 8 shows the calculated total  $(p,n)$  cross section; the points are the experimental  $(p,n)$  cross sections integrated over all angles and sum-

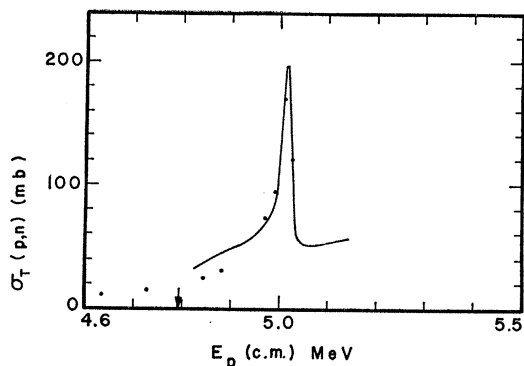


Fig. 8. The  $^{88}\text{Sr}(p,n)$  total cross section. The curve is the calculated result using Robson's theory. The points are the experimental data. See text for values of parameters used. The arrow refers to the threshold for the  $^{88}\text{Sr}(p,n_1)^{88}\text{Y}$  reaction.

med over the two open neutron channels. The complex potential parameters were taken from the work of Johnson *et al.*<sup>16</sup> and Moldauer.<sup>15</sup> The enhancement factor parameters used were  $E_0=5.015$  MeV,  $\Delta=-0.050$  MeV, and  $\Gamma=0.016$  MeV.

#### DISCUSSION AND CONCLUSIONS

The main purpose of the present work was to test the existing theories of isobaric analog resonances in  $(p,n)$  reactions. It is seen from Figs. 4, 5, 7, and 8 that, for this particular resonance in the  $^{88}\text{Sr}(p,n)$  reaction, both the coupled channel analysis and the  $R$ -matrix approach of Robson are in reasonably good agreement with experiment. Both theories reproduce the asymmetry in the resonance. Furthermore, they predict the

absence of the resonance in the  $^{88}\text{Sr}(p,n_1)$  reaction, which can be attributed to the lower transmission coefficient of the outgoing neutron leaving the residual nucleus in the first excited state. No correction for level width fluctuations have been made in the analyses, since the main purpose of the work was not to determine the complex potential parameters precisely, but to test the existing theories of analog resonances in  $(p,n)$  reactions.

It may be pointed out that the resonance width as given by the calculated compound-elastic cross section (15 keV) is less than the resonance width seen in the calculated  $(p,n)$  cross section illustrated in Fig. 4 ( $\sim 25$  keV). This difference has been experimentally observed. In the  $\text{Sr}^{88}+p$  reaction, the experimental width observed in the  $(p,n)$  reaction is 22 keV, whereas the width reported by Cosman *et al.*<sup>13</sup> from the  $^{88}\text{Sr}(p,p)$  work is 16 keV. This difference is due to the increased competition from proton reemission at the resonance, causing the  $(p,n)$  cross section to get depressed and hence increasing the width.

#### ACKNOWLEDGMENTS

The authors wish to thank Professor M. T. McEllistrem and Professor F. Gabbard for useful discussions during the course of this work. One of us (G.C.D.) would like to thank Professor B. D. Kern and Professor M. T. McEllistrem for providing the opportunity to work in the Nuclear Physics Laboratory of the University of Kentucky.

The numerical work was done at the University of Kentucky computing center and we are grateful to the staff of the center for their cooperation.